Carotenoids from Rhodomonas salina Induce Apoptosis and Sensitize A2058 Melanoma Cells to Chemotherapy

Raimundo Gonçalves de Oliveira-Júnior, Élodie Nicolau, Antoine Bonnet, Grégoire Prunier, Laureen Beaugeard, Nicolas Joguet, Valérie Thiéry, Laurent Picot

Carotenoids from *Rhodomonas salina* Induce Apoptosis and Sensitize A2058 Melanoma Cells to Chemotherapy

Raimundo Gonçalves de Oliveira-Júnior[1] · Elodie Nicolau[2] · Antoine Bonnet[1] · Grégoire Prunier[1] · Laureen Beaugeard[1] · Nicolas Joguet[3] · Valérie Thiéry[1] · Laurent Picot[1]

Received: 9 October 2019 / Accepted: 8 December 2019

Abstract

Melanoma is an aggressive tumor with invasive and metastatic potential, frequently exhibiting multidrug resistance mechanisms. In our continuous search for antimelanoma molecules, we have identified some effective marine compounds capable of not only inducing cell death, but also of sensitizing chemoresistant tumor cells to clinically used anticancer drugs. In this report, the cryptophyte *Rhodomonas salina* (Wislouch) D.R.A.Hill & R.Wetherbee, Pyrenomonadaceae, was chemically investigated in order to identify pigments efficiently inhibiting melanoma cells proliferation. All pharmacological tests were performed on A2058 cells expressing the oncogenic BRAF V600E mutation and resistant to dacarbazine treatment. Flash chromatography of *R. salina* ethanol extract led to purification of alloxanthin and crocoxanthin, which showed significant antiproliferative activity against A2058 cells, exhibiting IC_{50} = 29 and 50 μM, respectively. These carotenoids promoted growth inhibition, decreased cell migration, and induced apoptosis and sub-G1 cells accumulation after 72 h of treatment. In addition, alloxanthin potentiated the cytotoxic activity of vemurafenib (a BRAF inhibitor) and restored the sensitivity of A2058 cells to dacarbazine treatment.

Keywords Alloxanthin · Chemosensitivity · Crocoxanthin · Cutaneous melanoma · Drug resistance · Microalgae

Introduction

Cutaneous melanoma is an aggressive tumor deriving from melanocyte cells. In Europe, more than 20,000 people die from melanoma every year. It is the most frequent tumor in young adults aged 25 to 35 years old, and it is responsible for 70% of mortality by skin cancers (Schadendorf et al. 2018). The incidence of melanoma is increasing worldwide and most cases are associated with excessive exposure to UV radiation. In addition, advanced and metastatic melanoma (stages III and IV) have very poor prognosis and the overall positive responses to monotherapy using conventional anticancer drugs are weak, ranging from 4 to 26% (Matthews et al. 2017; Prado et al. 2019; Tracey and Vij 2019).

The classical antimelanoma drugs include alkylants agents (*e.g.*, dacarbazine, temozolomide, fotemustine, carmustine, semustine), platinum drugs (cisplatin and carboplatin), vinca alkaloids (vindezine and vinblastine), taxanes (docetaxel and paclitaxel), and tamoxifen (Garbe et al. 2016). Recently, promising results have been obtained with immunotherapy (monoclonal antibodies, *e.g.*, ipilimumab), target therapy (BRAF inhibitors, *e.g.*, vemurafenib; MEK inhibitors, *e.g.*, cobimetinib), and combined treatments (BRAF inhibitors associated to MEK inhibitors, *e.g.*, vemurafenib + cobimetinib) (Napolitano et al. 2018; Schadendorf et al. 2018). However, these treatments induce severe toxicity, including neutropenia, thrombocytopenia, fatigue, nausea, vomiting, and neurosensory troubles (Jang and Atkins 2014; Roos et al. 2014; Lopatka et al. 2018; Voskoboynik and Arkenau 2014). The wide range of antineoplastic treatments

✉ Laurent Picot
laurent.picot@univ-lr.fr

[1] Littoral Environnement et Sociétés (LIENSs, UMRi CNRS 7266), La Rochelle Université, La Rochelle, France

[2] Laboratoire Physiologie et Biotechnologie des Algues, Institut Français de Recherche pour l'Exploitation de la Mer, Nantes, France

[3] IDCAPS, R&D INNOV'IA, La Rochelle, France

ineffective at killing melanoma cells implies that the drug resistance mechanisms in melanoma are complex. In fact, melanoma cells are constitutively or adaptively resistant to pro-apoptotic drugs, acquiring mutations and cellular adaptations during the treatment that result in intrinsic survival mechanisms (Tentori et al. 2013; Spagnolo et al. 2014, 2015). Cytotoxic molecules usually lead to the selection of tumor cells variants overexpressing efflux transporters, such as P-glycoprotein (P-gp) and multidrug resistance factor-1 (MDR1), and anti-apoptotic proteins (*e.g.*, Bcl-2, Bcl-xL, Mcl-1), which justifies treatment failure (Housman et al. 2014).

Microalgae are a source of biomolecules considered not only promising dietary supplements (Gille et al. 2018), but also compounds that possess several therapeutic properties such as antioxidant, anti-inflammatory (Habashy et al. 2018), hypocholesterolemic (Sengupta et al. 2018), and anticancer (Juin et al. 2018). Among these compounds, a range of bioactive carotenoids can be isolated, including β-carotene, fucoxanthin, zeaxanthin, lutein, violaxanthin, echinenone, and canthaxanthin, and some of them are produced exclusively by microalgae (Casagrande et al. 2019). These pigments have often been associated with anticancer effects, including against cutaneous melanoma cell lines (Pasquet et al. 2011; Baudelet et al. 2013; Haguet et al. 2017). They exert antiproliferative effect by inducing apoptosis and modulating signaling pathways involved in survival, cell proliferation, invasion, and metastasis. Moreover, some carotenoids have been particularly investigated in combined treatments with drugs clinically used in melanoma therapy. In a recent study, we demonstrated that zeaxanthin isolated from *Porphyridium purpureum* sensitizes chemoresistant human melanoma cells to vemurafenib, enhancing its antiproliferative effect (Juin et al. 2018). Indeed, the use of natural molecules as sensitizer agents has been encouraged because of their low *in vivo* toxicity, allowing the reduction of effective doses of conventional anticancer drugs and consequently limiting potential toxic effects without affecting the therapeutic response (Vinod et al. 2013; de Oliveira Júnior et al. 2018).

In this report, we continue our search for new antimelanoma molecules through a chemical and pharmacological investigation of *Rhodomonas salina* (Wislouch) D.R.A.Hill & R.Wetherbee, Pyrenomonadaceae. It is a marine cryptophyte microalga, known to be rich in starch and routinely used in the diet of different invertebrate species (Tremblay et al. 2007; Chaloub et al. 2015). We have previously shown that chlorophyll c_2, alloxanthin, and β-carotene are the most common pigments found in *R. salina*, which makes it a promising source not only of nutrients but also of bioactive compounds (Serive et al. 2017). Nevertheless, many carotenoids remain unknown in this species and their anticancer potential has not yet been properly explored. In the present study, we describe the complete pigment profile of *R. salina* extract and the antiproliferative activity of two of its most promising carotenoids (alloxanthin and crocoxanthin) against chemoresistant human melanoma cells (A2058 cells) expressing the oncogenic BRAF mutation.

Materials and Methods

Microalgae Culture, Harvest, and Freeze-Drying

Rhodomonas salina (Wislouch) D.R.A.Hill & R.Wetherbee, Pyrenomonadaceae, CCAP 978/27 was grown in a commercial 16 l photobioreactor LUCY© (Synoxis algae, Le Cellier, France) containing 0.2-μm filtered and autoclaved seawater enriched with Walne's medium 4 ml l^{-1} (Walne 1970). The culture was realized in batch condition with a continuous irradiance of 120 μmol photons.m^{-2} s^{-1} photosynthetically active radiation (PAR) in a climate room at 18 °C. A pH 9 regulation was maintained with a regulated CO_2 injection. After 20 days, cells reached a concentration of 5.84×10^6 cell ml^{-1}. At this early stationary phase, 16 l of the culture were harvested by centrifugation. The microalgae paste was freezed at − 80 °C and freeze-dried before extraction. Additional information about the microalga species is available in the supplementary material.

Sonication-Assisted Extraction of *Rhodomonas salina* Pigments

Pigments were extracted from the lyophilized biomass (2 g) in absolute ethanol (500 ml). The mixture was sonicated at 50 W–30 kHz (UP50H ultrasonicator, Hielscher Ultrasonics GmbH, Germany) for 30 min, on ice and under constant stirring (Haguet et al. 2017). The extractive solution was filtered (PVDF 0.22-μm membrane) and the solvent was evaporated under vacuum, resulting in the *R. salina* extract (Rs-EtOH, 0.53 g).

Scanning Electron Microscopy

To confirm cell rupture during sonication-assisted extraction, *R. salina* cells were freeze-dried before or after sonication, placed on a conductive double layer carbon support and examined by SEM using a Philips-FEI Quanta 200 ESEM/ FEG microscope (environmental mode) equipped with a FEG canon delivering 1 to 30 kV beam current (Haguet et al. 2017).

UPLC-DAD-MS/MS Analysis

Pigment profile of Rs-EtOH was obtained by ultra-high performance liquid chromatography system (Acquity UPLC H-

class, Waters Milford USA) coupled to a photodiode array (Waters 2996) or a high-resolution mass spectrometry (XEVO G2S Q-TOF) equipped with an electrospray ionization source (Waters, Manchester, England). The UPLC system was formed by a quaternary pump (Quaternary Solvent Manager, Waters) and an automatic injector (Sample Manager-FTN, Waters) equipped with a 10 μl injection loop. 10 μl (DAD analysis) or 5 μl (MS analysis) of Rs-EtOH solution were injected in a C18 column (Acquity UPLC BEH C18, Waters) (2.1 × 50 mm, 1.7 μm), using a flow rate of 300 μl min^{-1} and a gradient composed of solvents A (water/formic acid, 100/0.001, v:v) and B (methanol/formic acid, 100/0.001, v:v), according to the following procedure: 0–1 min, 80% B; 1–2 min, 80%–81% B; 2–5 min, 81% B; 5–7 min, 81–81.5% B; 7–10 min, 81.5% B; 10–11 min, 81.5%–83% B; 11–14 min, 83% B; 14–16 min, 83%–85% B; 16–20 min, 85% B; 20–23 min, 85%–95% B; 23–27 min, 90% B; 27–29 min, 90%–95% B; 29–35 min, 95% B; 35–37 min, 95%–98% B; 37–43 min, 98% B; 43–44 min, 100% B; 44–48 min, 100% B; 48–48.5 min, 100%–20% B; 48.5–51 min, 20% B. During the analysis, the column and the injector were maintained at 25 °C and 7 °C, respectively. The instrument was adjusted for the acquisition on a 300–800-nm interval in UV mode, with 5 spectra s^{-1} and 1.2 nm of resolution. The analyses were performed in positive ionization mode with MSE function in a centroid mode. Final ESI conditions were source temperature 120 °C, desolvation temperature 500 °C, gas flow rate of the cone 50 l h^{-1}, desolvation gas flow rate 800 l h^{-1}, capillary voltage 3.0 kV, sampling cone 130 V, and source compensation 80 V. The instrument was set to acquire over the *m/z* 250–1300 *m/z* interval, with a scan time of 0.15 s. The mass spectrometer was calibrated before analysis using 0.5 mM sodium formate solution. Leucine Enkephalin (M = 555.62 Da, 1 ng μl^{-1}) was used as a lock-mass. UPLC-DAD

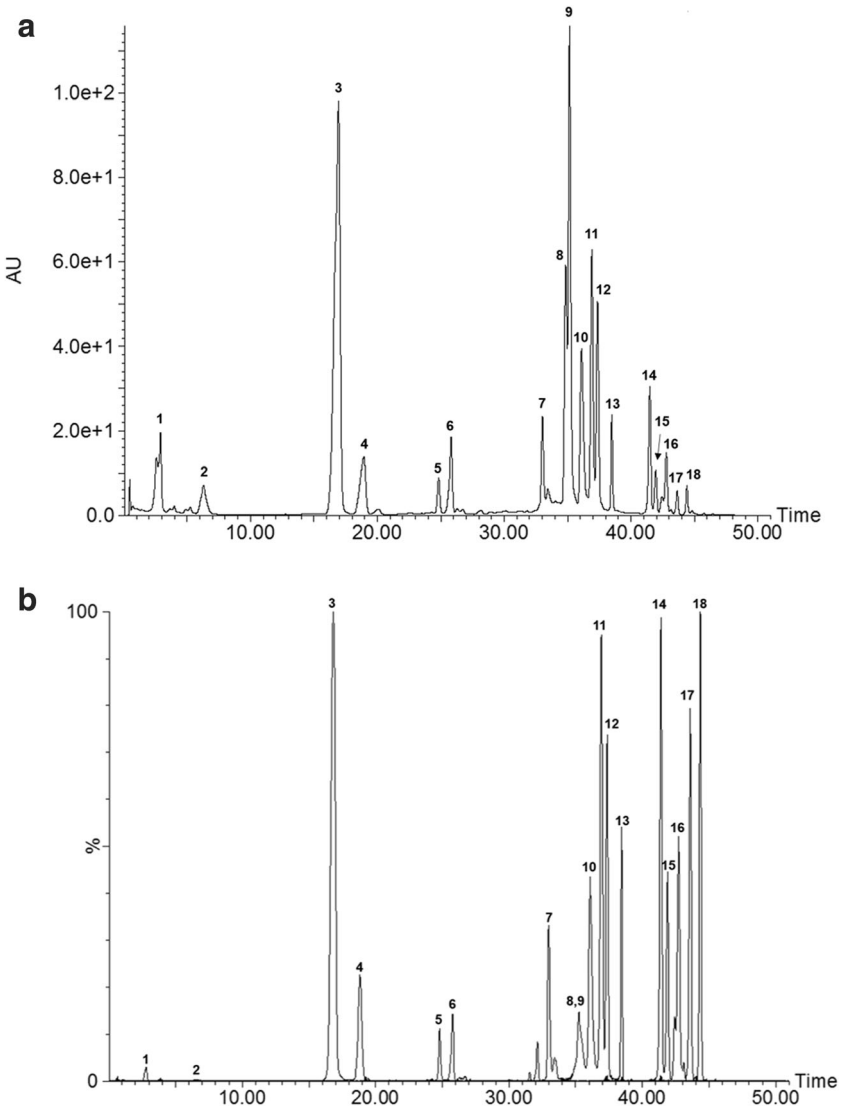

Fig. 1 UPLC-DAD (300–800 nm, full scan) (**a**) and UPLC-ESI-MS(+) (**b**) chromatograms of Rs-EtOH. Peak characterization is given in Table 1

Table 1 Identified pigments in Rs-EtOH by UPLC-DAD-MS/MS analysis. Peak number according to Fig. 1.

Peak	Pigment	RT (min)	Molecular formula	λ_{max} (nm)	Band III/II ratio (%)	Experimental *m/z* (Δ, ppm)			MS^2 fragments *m/z*
						$M^{\cdot+}$	$[M+H]^+$	$[M+Na]^+$	
1	Hydroxy-chlorophyll *c*2	2.81	$C_{35}H_{28}O_6N_4Mg$	452, 584, 634	-	-	-	647.1743 (2.1)	625.1926, 554.1555, 549.1735
2	Chlorophyll *c*2	6.47	$C_{35}H_{28}O_5N_4Mg$	452, 586, 635	-	-	609.1971 (2.8)	631.1799 (2.5)	549.1709
3	Alloxanthin	16.94	$C_{40}H_{52}O_2$	427, 451, 480	48.27	564.3970 (0.5)	-	587.3859 (1.0)	549.3735, 334.2290, 282.1976
4	Monadoxanthin	18.82	$C_{40}H_{54}O_2$	421, 445, 475	65.75	566.4122 (0.3)	-	589.4018 (0.0)	474.3481
5	Alloxanthin isomer	24.83	$C_{40}H_{52}O_2$	427, 451, 480	55.88	564.3970 (0.5)	-	587.3859 (1.0)	-
6	Alloxanthin isomer	25.82	$C_{40}H_{52}O_2$	427, 451, 480	29.00	564.3970 (0.5)	-	587.3859 (1.0)	-
7	Crocoxanthin	33.02	$C_{40}H_{54}O$	420, 444, 475	47.50	550.4179 (0.7)	-	-	535.3943, 494.3543, 458.3517, 119.0852
8	Hydroxy-chlorophyll *a*	34.72	$C_{55}H_{72}O_6N_4Mg$	421, 665	-	908.5294 (0.9)	-	-	630.2322
9	Hydroxy-chlorophyll *a* epimer	35.08	$C_{55}H_{72}O_6N_4Mg$	421, 665	-	908.5294 (0.9)	-	-	630.2322
10	Methoxylactone chlorophyll *a*	36.05	$C_{56}H_{74}O_7N_4Mg$	420, 651	-	938.5406 (0.2)	-	-	660.2441
11	Ethoxylactone chlorophyll *a*	36.93	$C_{57}H_{76}O_7N_4Mg$	421, 651	-	952.5565 (0.1)	-	-	-
12	Chlorophyll *a*	37.23	$C_{55}H_{72}O_5N_4Mg$	431, 661	-	892.5361 (0.9)	-	-	614.2377
13	Chlorophyll *a* epimer	38.48	$C_{55}H_{72}O_5N_4Mg$	412, 667	-	892.5340 (1.5)	-	-	614.2380
14	Hydroxy-pheophytin *a*	41.48	$C_{55}H_{74}O_6N_4$	407, 504, 533, 666	-	-	887.5677 (1.1)	-	609.2719
15	Hydroxy-pheophytin *a* epimer	41.95	$C_{55}H_{74}O_6N_4$	407, 504, 533, 666	-	-	887.5686 (0.1)	-	609.2719
16	β,ε-Carotene	42.78	$C_{40}H_{56}$	421, 441, 472	42.85	536.4390 (1.1)	-	-	444.3748
17	Pheophytin *a*	43.59	$C_{55}H_{74}O_5N_4$	408, 507, 538, 666	-	-	871.5743 (0.7)	-	593.2762
18	Pheophytin *a* epimer	44.34	$C_{55}H_{74}O_5N_4$	408, 507, 538, 666	-	-	871.5751 (1.6)	-	593.2766

RT retention time

chromatogram was recorded at 300–800 nm (full scan) and UPLC-MS/MS data were collected in positive mode (ESI^+). The mass error between experimental and theoretical parent and fragment ions was calculated as ([experimental m/z − theoretical m/z]/theoretical m/z) × 10^6 (ppm).

Purification of Alloxanthin and Crocoxanthin

Rs-EtOH was fractioned by flash liquid chromatography, using an Interchim Puriflash PF430 system. Rs-EtOH (100 mg) was solubilized in methanol and added to 10 g of celite® 545 (Sigma-Aldrich®, France). The mixture was homogenized manually until complete solvent evaporation and then placed in a pre-column. The pre-column containing Rs-EtOH-adsorbed celite® was coupled on the top of a PF-C18 column (20 g, 15 μm) and eluted with a mobile phase composed of a ternary solvent gradient: A (methanol/water, 80/20), B (acetonitrile/water, 90/10), and C (isopropanol). The gradient flow program was set as follows: 0–5 min, 100% A; 5–9 min, 100% B; 9–45 min, 30% B and 70% C; 45–50 min, 100% C; 50–55 min, 100% C; 55–60 min, 100% B; 60–65 min, 100% A; 65–70 min, 100% A. The flow rate was 5 ml min^{-1} and elution was monitored at 450 nm, with an automatic collector (10 ml per tube). This fractionation protocol was adapted from a previous study (Baudelet et al. 2013), considered an effective method for purification of microalgae pigments, especially carotenoids.

Cell Viability Assay

All pharmacological assays were performed using A2058 (ATCC® CRL-11147™) cell line. A2058 are highly invasive and metastatic human melanoma cells, BRAF-mutated (Ronca et al. 2013), tumorigenic at 100% frequency in nude mice (supplier's information) and very to conventional chemotherapy (de Oliveira Júnior et al. 2019). Cells were grown in DMEM (Dutscher, France), supplemented with 10% heat-inactivated (56 °C, 30 min) FCS (Dutscher, France) and penicillin-streptomycin (1000 U ml^{-1} and 100 μg ml^{-1}, respectively) (Dutscher, France), at 37 °C in a 5% CO_2 humidified atmosphere. Rs-EtOH and isolated carotenoids were solubilized in DMSO before dilution in the cell culture medium. The DMSO final concentration was lower than 1% and tested as negative control. A2058 cells (2×10^3/well) were treated with Rs-EtOH (1–100 μg ml^{-1}), alloxanthin (1–100 μM), or crocoxanthin (1–100 μM). After 72 h, cell viability was measured using the MTT assay as previously described (Mosmann 1983; Juin et al. 2018). Cell morphology was evaluated after treatments under inverted phase contrast microscope (Nikon, Eclipse, France). IC_{50} was calculated by non-linear regression analysis using Prism 6.0 (GraphPad Software).

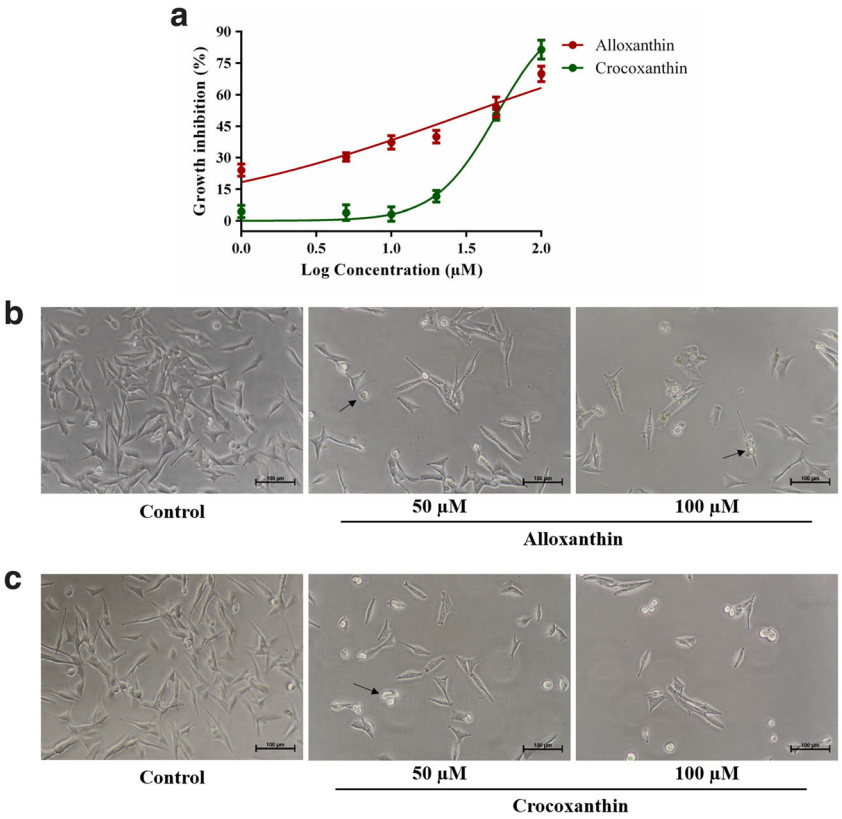

Fig. 2 Growth inhibition of A2058 cells after exposure to increasing concentrations (1–100 μM, 72 h) of alloxanthin and crocoxanthin (**a**). Treatments with alloxanthin and crocoxanthin evoked reduction in cell density, cell shrinkage, and rounding (black arrows) (**b**, **c**). Results are expressed as mean ± SEM, from at least three independent measurements ($n = 3$)

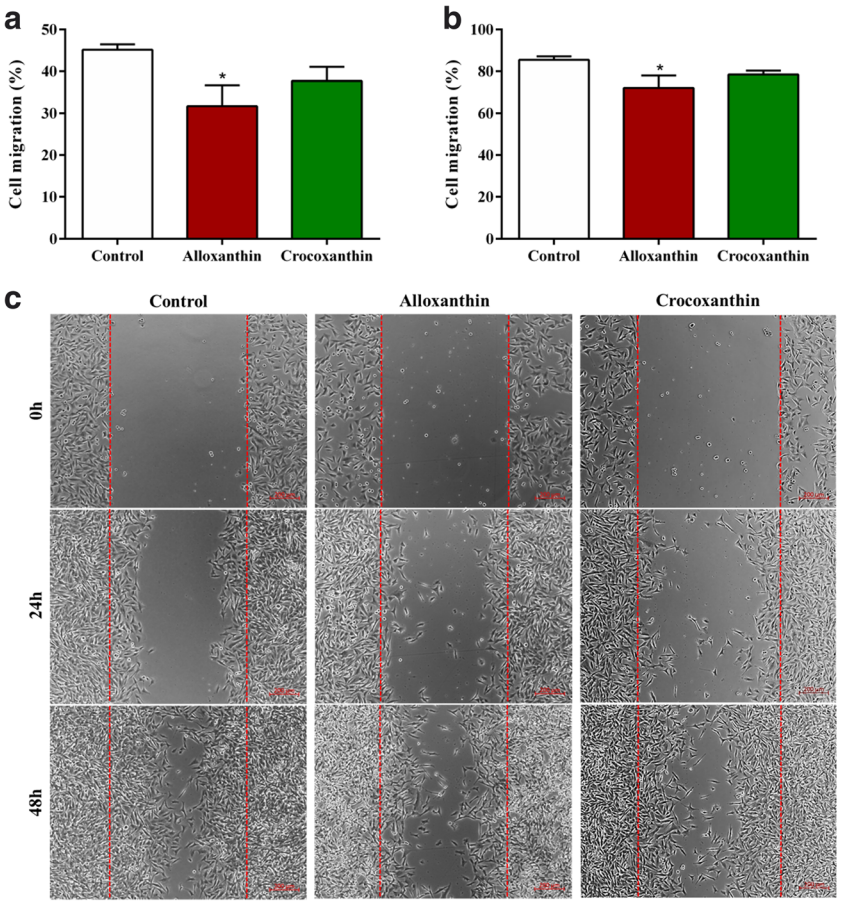

Fig. 3 Antimigratory activity of alloxanthin (14.5 μM, ½IC_{50}) and crocoxanthin (25 μM, ½IC_{50}) after 24 h (**a**) and 48 h (**b**) of exposure. Photomicrographs represent cell migration into the zone free of cells according to the treatment (**c**). Data are expressed as mean ± SEM, $*p < 0.05$ (one-way ANOVA followed by Tukey's post-test), from at least three independent measurements ($n = 3$)

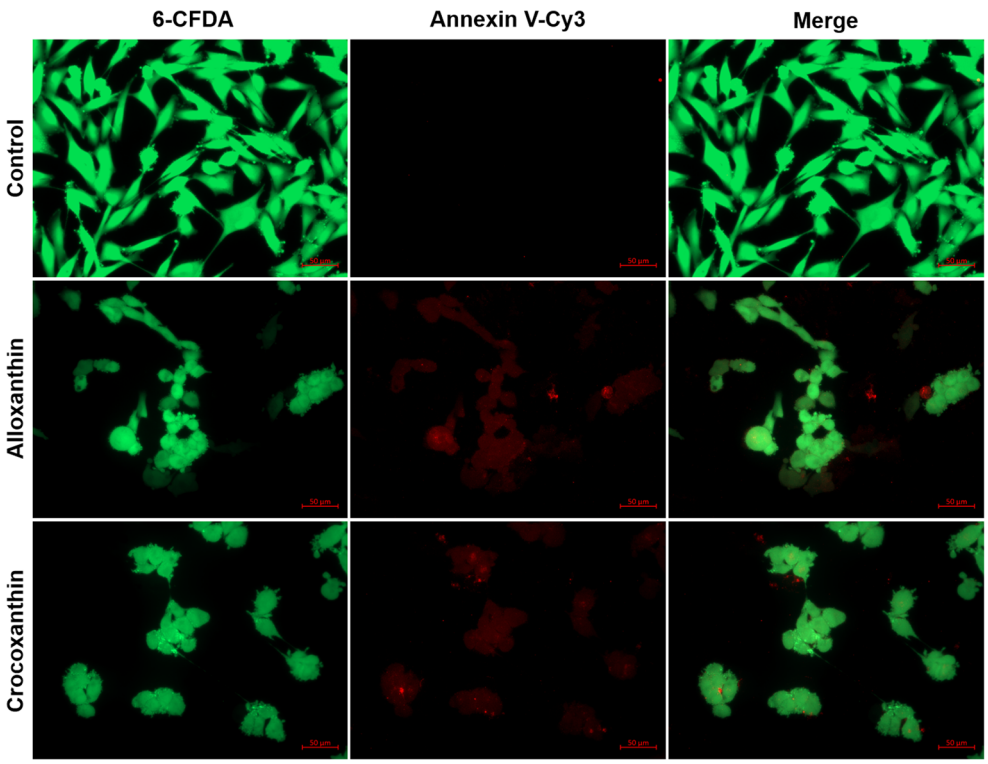

Fig. 4 Alloxanthin (29 μM, IC_{50}) and crocoxanthin (50 μM, IC_{50}) induce apoptosis in A2058 cells, after 72 h of treatment. Annexin V (red) and 6-CFDA (green) double staining was observed by fluorescence microscopy. Melanoma cells in early apoptosis show both red and green stains, while cells in late apoptosis show only red stain, and untreated cells (control) are stained green only. Treated cells also presented cell shrinkage and rounding, cell clumps, and apoptotic bodies formation

Cell Migration Assay

Antimigratory activity of alloxanthin and crocoxanthin was determined as previously reported (Cisilotto et al. 2018). A2058 cells (2×10^4/well) were incubated and grown to 90% confluence in 24-well plates. Cell monolayers were scratched with a sterile plastic tip, washed with PBS and incubated in a fresh cell culture medium containing alloxanthin (14.5 μM, ½IC_{50}) or crocoxanthin (25 μM, ½IC_{50}), for 48 h. Cell migration was microscopically monitored at 0, 24, and 48 h (ZEISS Axion Observer, France), and results were expressed as percentage of cell migration calculated by measuring the cell surface using ImageJ® software.

Annexin V-Cy3/6-CFDA Analysis

Cells were incubated for 24 h and subsequently treated with alloxanthin (29 μM, IC_{50}) or crocoxanthin (50 μM, IC_{50}). After 72 h of treatment, cells were washed with PBS and double stained with annexin V-Cy3 (red fluorescence) and 6-carboxyfluorescein diacetate (6-CFDA, green fluorescence) solution according to manufacturer's recommendations (Sigma-Aldrich®, France) and finally observed under fluorescent microscope (ZEISS Axion Observer, France) (de Oliveira Júnior et al. 2019).

Nuclear Fragmentation

Cells were incubated for 24 h in 4-well chamber slides (5000 cells/well) and then treated with alloxanthin (29 μM, IC_{50}) or crocoxanthin (50 μM, IC_{50}) for 72 h. Cells were washed in PBS before being fixed with formaldehyde 4% solution for 30 min at 37 °C. Subsequently, cells were washed in PBS, permeabilized with Triton X-100 1% and finally stained with DAPI according to manufacturer's instructions (ProLong™ Gold Antifade Mountant with DAPI kit, ThermoFischer Scientific, France). Nuclear condensation and fragmentation of untreated and treated cells were observed under fluorescent microscope (ZEISS Axion Observer, France).

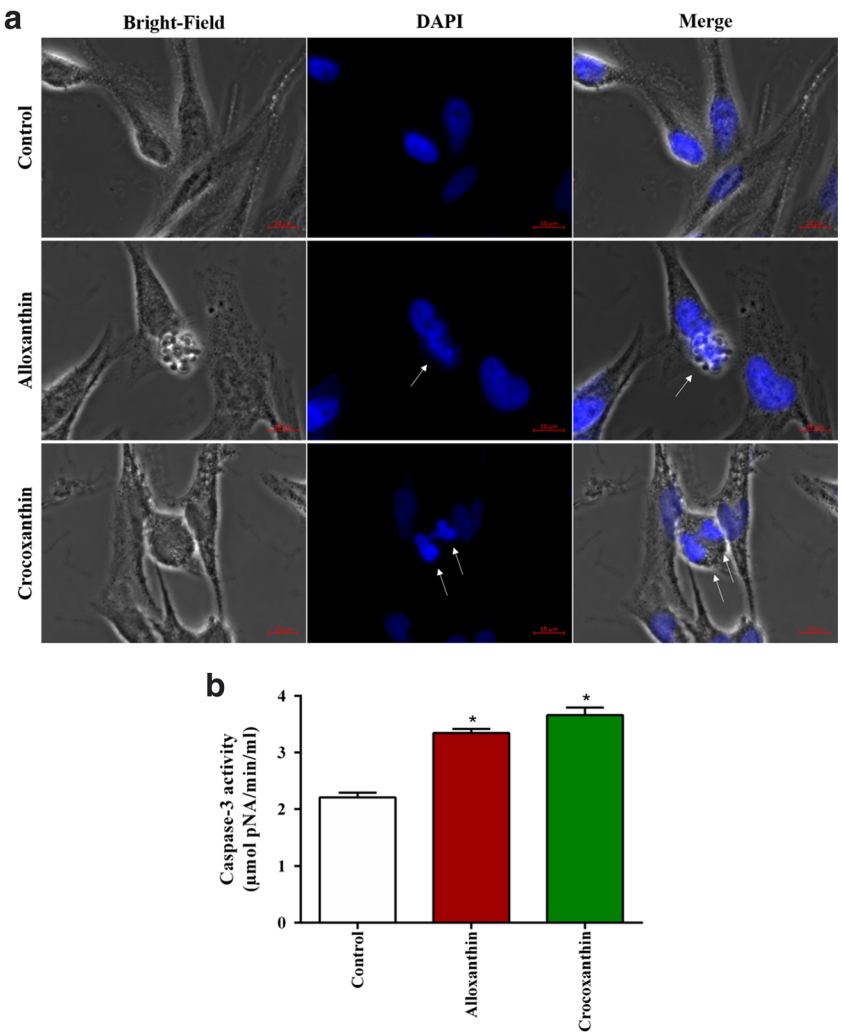

Fig. 5 Nuclear fragmentation (**a**) and caspase-3 activation (**b**) in A2058 cells exposed to alloxanthin (29 μM, IC_{50}) and crocoxanthin (50 μM, IC_{50}) during 72 h of treatment. Arrows point Blebbing, DNA condensation, and fragmentation after DAPI staining (**a**). Enzymatic activity (μmol pNA/min/ml) is expressed as mean ± SEM (**b**), with $*p < 0.05$ (vs. control group), according to one-way ANOVA followed by Tukey's post-test ($n = 3$)

Caspase-3 Activity

Caspase-3 activity was determined using a colorimetric assay (CASP3C kit, Sigma-Aldrich®, France) as previously reported. Cells were treated with alloxanthin (29 μM, IC_{50}) or crocoxanthin (50 μM, IC_{50}) for 72 h. After treatment, cells were washed with PBS, lysed with lysis buffer, and caspase-3 activity (μmol pNA/min/ml) was measured according to manufacturer's instructions.

Cell Cycle Analysis

A2058 cells were treated with alloxanthin (29 μM, IC_{50}) or crocoxanthin (50 μM, IC_{50}) for 72 h before being stained with PBS containing propidium iodide (PI 100 μg ml^{-1}), Rnase A (100 μg ml^{-1}) and 0.1% Triton X-100 (ThermoFisher Scientific, France) for 15 min, at 37 °C. Cells were analyzed using a FACS Cantoll flux cytometer (BD Biosciences, France) equipped with an air cooled blue LASER ($\lambda = 488$ nm, 20 mW) as previously described (Juin et al. 2018).

Sensitization of A2058 Cells to Vemurafenib and Dacarbazine

Vemurafenib (Selleckchem®, France) and dacarbazine (Sigma-Aldrich®, France) were diluted to a 10 mM stock solution in PBS, before dilution in cell culture medium. A2058 cells were treated for 72 h with increasing concentrations of vemurafenib (1–100 μM) or dacarbazine (1–100 μM), alone or combined to alloxanthin (14.5 μM, ½IC_{50}) or crocoxanthin (25 μM, ½IC_{50}). Antiproliferative activity of monotherapies and combined therapies was calculated using MTT assay as described above and results were expressed as IC_{50}. The combination index (CI) was calculated using the software CompuSyn (version 1.0), according to Chou-Talalay method (Chou and Talalay 1984). CI < 1.0 indicates synergism, CI > 1.0 indicates antagonism, and CI values equal to 1.0 indicate additive effect.

Statistical Analysis

Data were expressed as mean ± SEM and analyzed by unpaired Student's *t* test or one-way ANOVA followed by

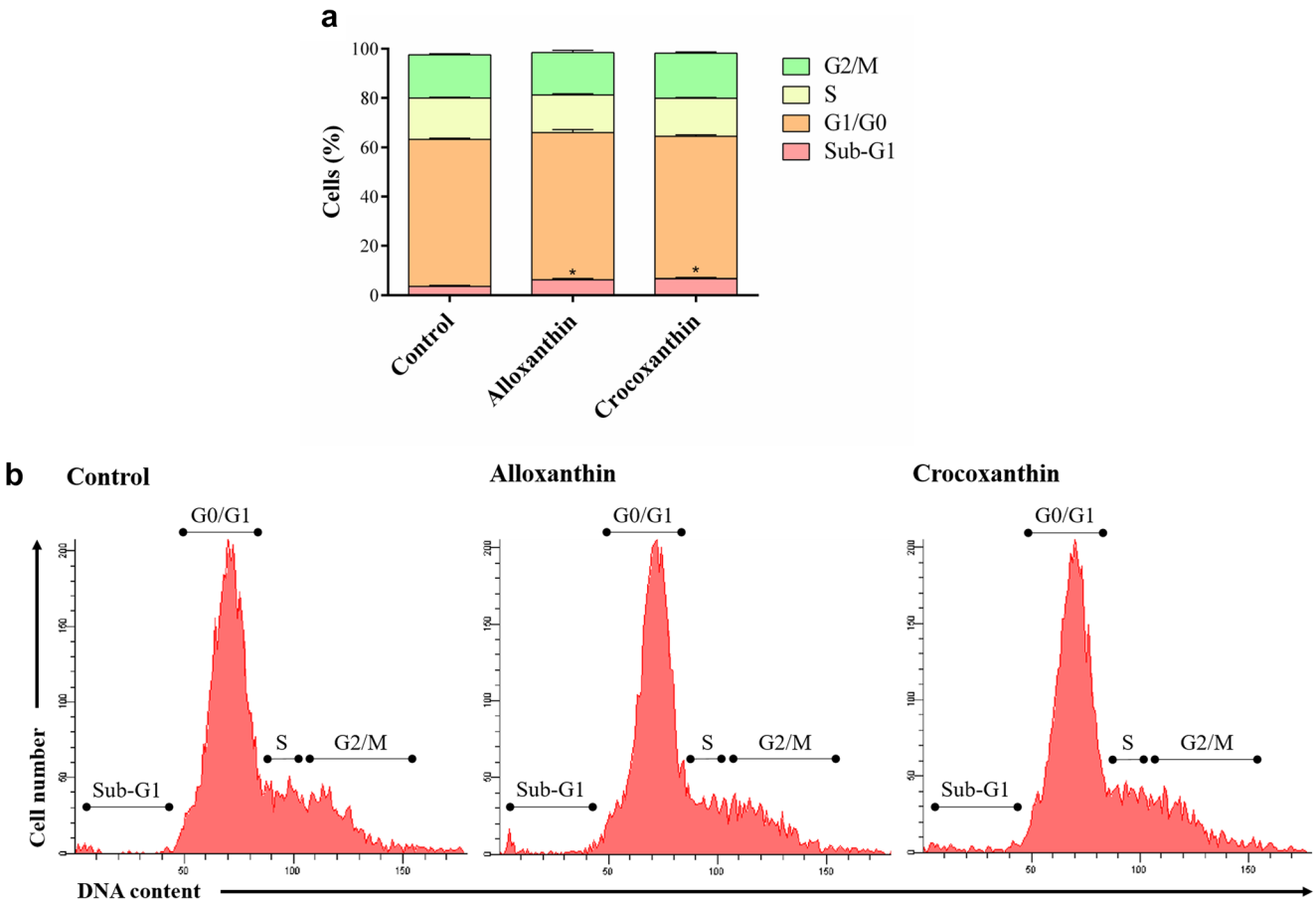

Fig. 6 Effect of alloxanthin (29 μM, IC_{50}) and crocoxanthin (50 μM, IC_{50}) on different phases of cell cycle (Sub-G1, G1/G0, S, G2/M). A2058 cells were treated for 72 h, stained with propidium iodide, and measured by flow cytometry, as shown in the quantitative distribution of cells in different phases of cell cycle (**a**) and in the representative histograms (**b**). Data are expressed as mean ± SEM, $^*p < 0.05$ (vs. control group) according to one-way ANOVA followed by Tukey's post-test, from at least three independent measurements ($n = 3$)

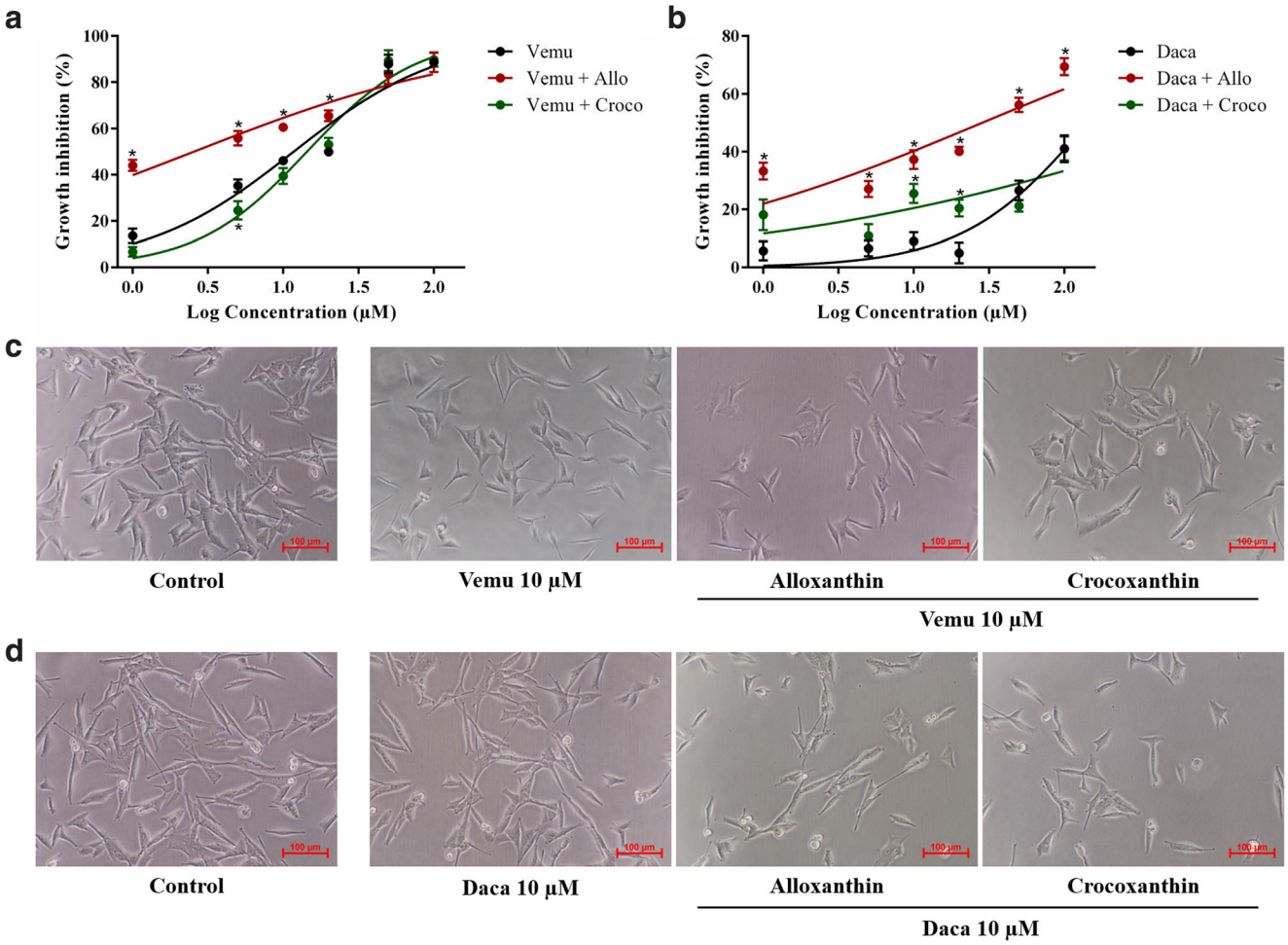

Fig. 7 Antiproliferative activity of alloxanthin (allo, 14.5 μM) and crocoxanthin (croco, 25 μM) combined with vemurafenib (vemu) (**a**) and dacarbazine (daca) (**b**) in the MTT assay. A2058 cells were grown for 72 h with increasing concentrations of the anticancer drugs (1–100 μM) in the presence or absence of the carotenoids (½IC_{50}). Photomicrographs show reduction of cell density promoted by combined therapies, compared with monotherapies and control groups (**c**). Data are expressed as mean ± SEM, *$p < 0.05$ according to unpaired Student's *t* test, from at least three independent measurements ($n = 3$)

Tukey's multiple comparison test (statistical significance when $p < 0.05$), according to the case, using Prism 6.0 (GraphPad software). Pharmacological results were obtained from at least three independent measurements ($n = 3$ or more).

Table 2 Antiproliferative activity of monotherapies and combined therapies against A2058 cells. Data are presented as IC_{50} values and 95% confidence interval. For combined therapy, increasing concentrations of vemurafenib and dacarbazine (1–100 μM) were associated to ½IC_{50} of alloxanthin (14.5 μM) and crocoxanthin (25 μM)

Monotherapy	IC_{50} (μM)	Combined therapy	IC_{50} (μM)
Allo	29.16 (21.56–39.45)	-	-
Croco	49.92 (45.21–55.12)	-	-
Vemu	11.71 (10.09–13.58)	Vemu + Allo (½ IC_{50})	2.54 (1.76–3.66)
		Vemu + Croco (½ IC_{50})	14.35 (12.48–16.51)
Daca	> 100	Daca + Allo (½ IC_{50})	28.31 (20.62–38.86)
		Daca + Croco (½ IC_{50})	> 100

Allo alloxanthin, *croco* crocoxanthin, *vemu* vemurafenib, *daca* dacarbazine. IC_{50} is defined as the concentration of a compound inhibiting 50% of cell growth, calculated by non-linear regression. ½IC_{50} correspond to half of the IC_{50} value. Data are expressed as mean (95% confidence intervals), from at least three independent measurements ($n = 3$)

Results and Discussion

Sonication-Assisted Extraction of *Rhodomonas salina* Pigments

Microalgae have hard cell wall in most of cases, which limits metabolites extraction by conventional methods. Accordingly, sonication-assisted extraction has been increasingly used to obtain compounds from different microalgae as previously demonstrated by our research group (Baudelet et al. 2013; Juin et al. 2015; Haguet et al. 2017). To ensure complete extraction of pigments, *R. salina* freeze-dried biomass was sonicated for 30 min at 50 W-30 kHz, using ethanol as solvent. Scanning electron microscopy of freeze-dried biomass before sonication revealed cells with intact cell morphology. In contrast, *R. salina* cells showed cell wall disruption after sonication-assisted extraction, allowing the direct contact of the solvent with the intracellular content (supplementary data).

Pigment Profile of *Rhodomonas salina* Extract (Rs-EtOH)

UPLC-DAD-MS/MS analysis of Rs-EtOH was achieved in a single 51-min run and eighteen peaks were identified according to their UV, MS, and MS/MS spectral data (Fig. 1 and Table 1). Chlorophylls c_2 and *a*, pheophytin *a*, and the carotenoids alloxanthin, monadoxanthin, crocoxanthin, and β,ε-carotene were the main pigments identified, corroborating previous chemical investigation involving *R. salina* (Kaňa et al. 2012; Vu et al. 2016; Serive et al. 2017). Alloxanthin, monadoxanthin, and crocoxanthin are carotenoids of frequent occurrence in the *Rhodomonas* genus, since they have been reported in *R. baltica*, *R. lens*, and *R. minuta* (Zapata et al. 2000; Teubner et al. 2003; Sanz et al. 2015; van Houcke et al. 2017). Chlorophyll c_2, chlorophyll *a*, and pheophytin *a* derivatives (hydroxyl, methoxylactone, and ethoxylactone forms) were also detected. Although these derivatives are naturally occurring in microalgae (Hynninen 1981; Baudelet et al. 2013; Juin et al. 2015; Haguet et al. 2017), they may have originated during the extraction procedure due to the high chlorophyll instability. Chemical structures of the main identified molecules are presented in supplementary data.

Antiproliferative Activity of Rs-EtOH

The antiproliferative activity of Rs-EtOH against A2058 cells was also evaluated. Rs-EtOH induced a concentration-dependent reduction of cell viability when compared with the control group, reaching 38.81 ± 2.70% growth inhibition at the maximum concentration tested (100 μg ml^{-1}). The IC_{50} estimated to Rs-EtOH was > 100 μg ml^{-1}, indicating a weak antiproliferative effect (supplementary data). However, the Rs-EtOH composition includes carotenoids unpreviously investigated for their anticancer potential, such as alloxanthin and crocoxanthin. Therefore, we fractionated Rs-EtOH in order to evaluate the antiproliferative effect of its isolated pigments.

Purification and Characterization of Alloxanthin and Crocoxanthin

Flash liquid chromatography fractionation of Rs-EtOH (100 mg) led to the achievement of ten fractions (F1-F10), collected according to their UV absorption in a 450-nm monitored elution (supplementary data). After UPLC-DAD-MS/MS analysis, F5 and F8 were identified as alloxanthin (**1**) (4.2 mg) and crocoxanthin (**2**) (1.2 mg), respectively. All experimental spectral data (supplementary data) were in accordance with literature (Baudelet et al. 2013; Rodriguezl 2000; Sanz et al. 2015), and carotenoid purity grade was > 95% (UPLC-DAD chromatogram, 300–800 nm). Subsequently, we evaluated the antiproliferative activity of alloxanthin and crocoxanthin against melanoma cells.

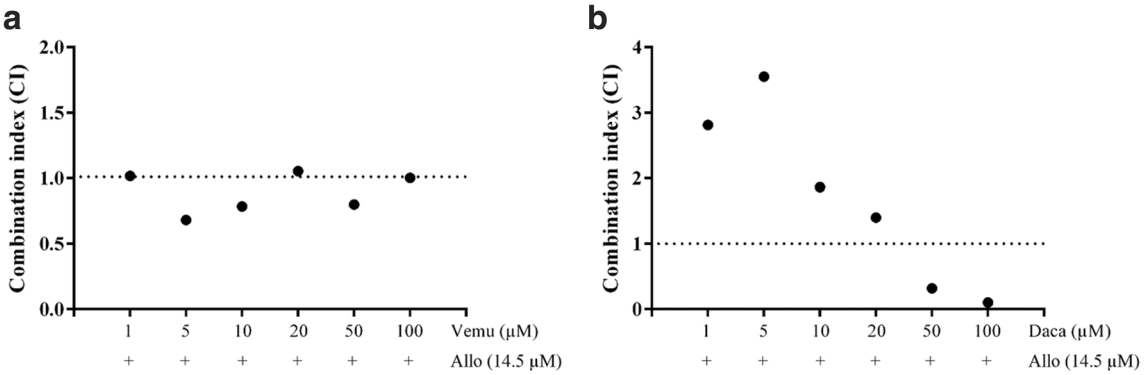

Fig. 8 Combination index (CI) for the association of alloxanthin (14.5 μM, ½IC_{50}) with vemurafenib (1–100 μM) (**a**) or dacarbazine (1–100 μM) (**b**) in the MTT assay (72 h of treatment), calculated according to data shown in Table 2. CI = 1 indicates additive effect, CI < 1 indicates synergism, and CI > 1 indicates antagonism, according to Chou-Talalay method (Chou and Talalay 1984)

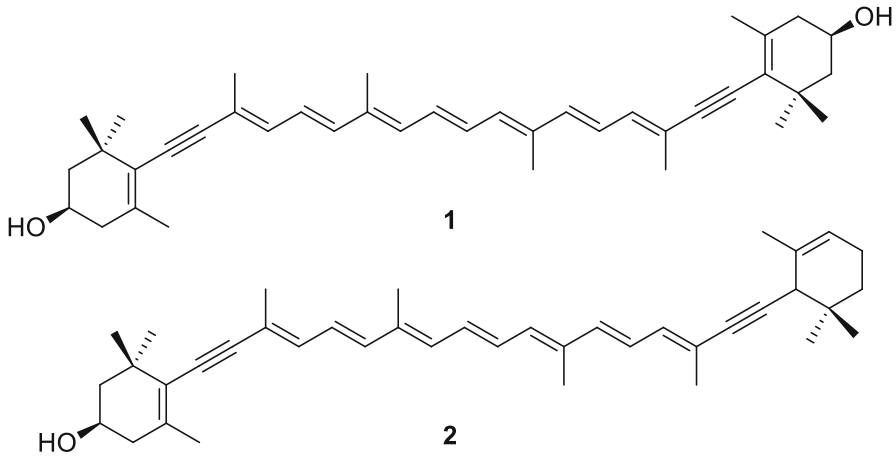

Alloxanthin and Crocoxanthin Inhibit Proliferation of A2058 Cells

Alloxanthin and crocoxanthin (1–100 μM) induced a concentration-dependent reduction in the number of A2058 cells when compared with the control group, showing IC_{50} of 29 and 50 μM, respectively (Fig. 2). Untreated cells exhibited regular epithelial morphology and became sub-confluent after 72 h, indicating a high proliferation rate. In contrast, alloxanthin and crocoxanthin (50 and 100 μM) treatments induced reduction in cell density, cell shrinkage, and appearance of rounding cells (black arrows) (Fig. 2).

Alloxanthin Inhibits Cell Migration

In the cell migration assay, alloxanthin (14.5 μM, ½IC_{50}) decreased cell migration into the zone free of cells (Fig. 3) after 24 h and 48 h of exposure. However, crocoxanthin (25 μM, ½IC_{50}) did not significantly suppress cell migration compared with control cells.

Pro-apoptotic Effect of Alloxanthin and Crocoxanthin

Several *in vitro* and *in vivo* studies have shown that the anticancer activity of carotenoids involves multiple mechanisms, including suppression of cell proliferation and mobility, and induction of apoptosis (Sathasivam and Ki 2018; Sugawara et al. 2014; Wang et al. 2014). In fact, modulation of pro-apoptotic pathways is a major biochemical response promoted by carotenoids. Typically, carotenoids up regulate the expression of important pro-apoptotic proteins (*e.g.*, Bad, Bax, Bid, Bim), while decrease the expression of anti-apoptotic targets (*e.g.*, Bcl-xL, Bcl-2), resulting in cell death (Juin et al. 2018; Kumar et al. 2013). In this paper, the pro-apoptotic effect of alloxanthin (29 μM, IC_{50}) and crocoxanthin (50 μM, IC_{50}) on A2058 cells was also investigated. After 72 h of exposure, the number of Annexin V and 6-CFDA double-stained cells (early apoptotic cells) was expressively increased for both treatments when compared with untreated cells. In addition, alloxanthin- and crocoxanthin-treated cells showed significant morphological changes, such as cell shrinkage and rounding, and tendency to form cell clumps and apoptotic bodies (Fig. 4).

Caspase-3 activation displays an important role in cell death via the intrinsic and extrinsic apoptosis pathways. Caspase-3 is a final executor caspase, responsible for apoptotic chromatin condensation and DNA fragmentation, resulting in cell dismantling and formation of apoptotic bodies (Porter and Ja 1999). In this context, we evaluated the effect of alloxanthin (29 μM) and crocoxanthin (50 μM) on caspase-3 activity and nuclear fragmentation through enzymatic assay and DAPI staining, respectively. As shown in Fig. 5, both carotenoids induced a significant increase in caspase-3 activity after 72 h of treatment. In addition, treated cells showed blebbing, DNA condensation and fragmentation (Fig. 5) compared with untreated cells, confirming the pro-apoptotic effect of alloxanthin and crocoxanthin in melanoma cells.

Alloxanthin and Crocoxanthin Induce Accumulation of Sub-G1 Cells

Flow cytometry analysis revealed a significant increasing in sub-G1 cell population after exposure to alloxanthin (29 μM, IC_{50}) and crocoxanthin (50 μM, IC_{50}), characteristic of dying cells (Fig. 6). Quantitative analysis using BD FACS Diva Software indicated 3.60 ± 0.44% of control cells were in sub-G1 phase in comparison with 6.30 ± 0.43 and 6.72 ± 0.43% of alloxanthin- and crocoxanthin-treated cells, respectively ($p < 0.05$) (Fig. 6). This result corroborates the pro-apoptotic effect observed previously for both molecules, without affecting the other cell cycle phases.

Alloxanthin Sensitizes A2058 Cells to Chemotherapy

Due to their metastatic and chemoresistant potential (de Oliveira Júnior et al. 2019), A2058 cells represent a good cell model to evaluate the chemosensitizing effect of cytostatic agents. They express the oncogenic BRAF V600E mutation, present in 40–70% of clinical cases (Flaherty and McArthur 2010). Although target therapies using BRAF inhibitors (*e.g.*, vemurafenib) have improved the treatment of metastatic melanoma, most patients develop resistance mechanisms that limit therapeutic efficacy (Chapman et al. 2011; Chakraborty et al. 2013; Tentori et al. 2013). In this sense, we evaluated the chemosensitizing effect of *R. salina* carotenoids using the MTT assay. Alloxanthin and crocoxanthin (½IC_{50}) were combined with increasing concentrations of vemurafenib (BRAF inhibitor) or dacarbazine (alkylating agent), and tested for 72 h. As shown in Fig. 7, A2058 cells were sensitive to vemurafenib (IC_{50} = 11.71 μM) but resistant to dacarbazine (IC_{50} > 100 μM). Crocoxanthin was not able to potentiate the antiproliferative activity of both anticancer drugs. However, alloxanthin enhanced the antiproliferative effect of vemurafenib by reducing its IC_{50} from 11.71 to 2.54 μM. Furthermore, alloxanthin restored the sensitivity of melanoma cells to dacarbazine (IC_{50} = 28.31 μM for combined treatment) (Table 2), reducing significantly cell density compared with monotherapy (Fig. 7).

In order to better characterize the sensitizing effect of alloxanthin, combination index (CI) was calculated for combined therapies (alloxanthin + vemurafenib and alloxanthin + dacarbazine) using the Chou-Talalay method (Chou and Talalay 1984). CI values were used to check whether the antiproliferative effect was due to an additive (CI = 1), synergistic (CI < 1), or antagonistic (CI > 1) effect. As shown in Fig. 8, alloxanthin + vemurafenib combination resulted in a synergistic effect at 14.5 + 5, 14.5 + 10, and 14.5 + 50 μM treatments, while alloxanthin + dacarbazine treatment resulted in a synergistic effect at the highest concentrations (14.5 + 50 or 100 μM, respectively). In this sense, alloxanthin contributes to the antiproliferative effect of vemurafenib and dacarbazine, and may cooperate to reduce resistance in melanoma cells expressing BRAF mutation.

Conclusion

This report establishes for the first time a complete pigment profile of *R. salina*, a cryptophyte microalga widely used in aquaculture and possessing an invaluable interest in the pharmaceutical and nutraceutical sectors. Alloxanthin and crocoxanthin were identified as promising antiproliferative molecules against chemoresistant melanoma cells. These carotenoids limit growth inhibition, reduce cell migration, and induce apoptosis and accumulation of sub-G1 cells. In addition, alloxanthin potentiates the antiproliferative activity of vemurafenib, a BRAF inhibitor, and restores the sensitivity of A2058 cells to dacarbazine, a conventional alkylating agent commonly used for melanoma treatment. Although further and in-depth investigations are needed, the present study demonstrates that marine carotenoids may be used as adjuvants, improving the sensitivity of melanoma cells to chemotherapy.

Acknowledgments We thank Thierry Beignon from Synoxis Algae Company (Le Cellier, France) for the loan of LUCY photobioreactor.

Authors' Contributions EN produced *R. salina* biomass; RGOJ and AB performed pigments extraction, purification and characterization by UPLC-DAD-MS/MS analysis; RGOJ, GP, LB and LP performed all pharmacological tests (cell culture, fluorescence microscopy, live cell imaging, flow cytometry, etc.); RGOJ and NJ performed SEM analysis; RGOJ and VT participated in the design of the manuscript, data analysis and interpretation and in the writing process; LP supervised the entire study in collaboration with VT and EN.

Funding Information This research was financially supported by the INTERREG Atlantic Area European program (Interreg EnhanceMicroAlgae project, EAPA_338/2016), and the French cancer league (Comité 17 de la Ligue Nationale contre le Cancer).

Compliance with Ethical Standards

Conflict of Interest The authors declare that they have no conflict of interest.

Protection of Human and Animal Subjects The authors declare that no experiments were performed on humans or animals for this study.

Confidentiality of Data The authors declare that no patient data appear in this article.

Right to Privacy and Informed Consent The authors declare that no patient data appear in this article.

References

Baudelet PH, Gagez AL, Bérard JB, Juin C, Bridiau N, Kaas R, Thiéry V, Cadoret JP, Picot L (2013) Antiproliferative activity of Cyanophora paradoxa pigments in melanoma, breast and lung cancer cells. Mar Drugs 11:4390–4406. https://doi.org/10.3390/md11114390

Casagrande T, Cazarin CBB, Marostica MR Jr, Risso ÉM, Amaya-Farfan J, Grimaldi R, Mercadante AZ, Jacob-Lopes E, Zepka LQ (2019) Microalgae biomass intake positively modulates serum lipid profile and antioxidant status. J Funct Foods 58:11–20. https://doi.org/10.1016/j.jff.2019.04.047

Chakraborty R, Wieland CN, Comfere NI (2013) Molecular targeted therapies in metastatic melanoma. Pharmgenomics Pers Med 6:49–56. https://doi.org/10.2147/PGPM.S44800

Chaloub RM, Motta NMS, de Araujo SP, de Aguiar PF, da Silva AF (2015) Combined effects of irradiance, temperature and nitrate concentration on phycoerythrin content in the microalga Rhodomonas sp. (cryptophyceae). Algal Res 8:89–94. https://doi.org/10.1016/j.algal.2015.01.008

Chapman PB, Hauschild A, Robert C, Haanen JB, Ascierto P, Larkin J, Dummer R (2011) Improved survival with vemurafenic in

melanoma with BRAF V600E mutation. N Engl J Med 364:2507–2516. https://doi.org/10.1056/NEJMoa1103782

Chou T, Talalay P (1984) Quantitative dose-effect relationships: the combined effects of multiples drugs or enzyme inhibitors. Adv Enzym Regul 22:27–55. https://doi.org/10.1016/0065-2571(84)90007-4

Cisilotto J, Sandjo LP, Faqueti LG, Fernandes H, Joppi D, Biavatti MW, Creczynski-Pasa TB (2018) Cytotoxicity mechanisms in melanoma cells and UPLC-QTOF/MS2chemical characterization of two Brazilian stingless bee propolis: uncommon presence of piperidinic alkaloids. J Pharm Biomed Anal 149:502–511. https://doi.org/10.1016/j.jpba.2017.11.038

de Oliveira Júnior RG, Bonnet A, Braconnier E, Groult H, Prunier G, Beaugeard L, Grougnet R, da Silva Almeida JRG, Ferraz CAA, Picot L (2019) Bixin, an apocarotenoid isolated from Bixa orellana L, sensitizes human melanoma cells to dacarbazine-induced apoptosis through ROS-mediated cytotoxicity. Food Chem Toxicol 125:549–561. https://doi.org/10.1016/j.fct.2019.02.013

de Oliveira Júnior RG, Christiane Adrielly AF, da Silva Almeida JRG, Grougnet R, Thiéry V, Picot L (2018) Sensitization of tumor cells to chemotherapy by natural products: a systematic review of preclinical data and molecular mechanisms. Fitoterapia 129:383–400. https://doi.org/10.1016/j.fitote.2018.02.025

Flaherty KT, McArthur G (2010) BRAF, a target in melanoma. Cancer 116:4902–4913. https://doi.org/10.1002/cncr.25261

Garbe C, Peris K, Hauschild A, Saiag P, Middleton M, Bastholt L, Grob J, Malvehy J (2016) Diagnosis and treatment of melanoma. European consensus-based interdisciplinary guideline - update 2016. Eur J Cancer 63:201–217. https://doi.org/10.1016/j.ejca.2016.05.005

Gille A, Neumann U, Louis S, Bischo SC, Briviba K (2018) Microalgae as a potential source of carotenoids: comparative results of an *in vitro* digestion method and a feeding experiment with C57BL/6J mice. J Funct Foods 49:285–294. https://doi.org/10.1016/j.jff.2018.08.039

Habashy NH, Abu MM, Attia WE, Abdelgaleil SAM (2018) Chemical characterization, antioxidant and anti-inflammatory properties of Greek Thymus vulgaris extracts and their possible synergism with Egyptian Chlorella vulgaris. J Funct Foods 40:317–328. https://doi.org/10.1016/j.jff.2017.11.022

Haguet Q, Bonnet A, Bérard JB, Goldberg J, Joguet N, Fleury A, Thiéry V, Picot L (2017) Antimelanoma activity of Heterocapsa triquetra pigments. Algal Res 25:207–215. https://doi.org/10.1016/j.algal.2017.04.034

Housman G, Byler S, Heerboth S, Lapinska K, Longacre M, Snyder N, Sarkar S (2014) Drug resistance in cancer: an overview. Cancers 6:1769–1792. https://doi.org/10.3390/cancers6031769

Hynninen PH (1981) Mechanism of the Allomerization of chlorophyll: inhibition of the allomerization by carotenoid pigments. Z Naturforsch 36b:1010–1016

Jang S, Atkins MB (2014) Treatment of BRAF-mutant melanoma: the role of vemurafenib and other therapies. Clin Pharmacol Ther 95:24–31. https://doi.org/10.1038/clpt.2013.197

Juin C, Bonnet A, Nicolau E, Bérard JB, Devillers R, Thiéry V, Cadoret JP, Picot L (2015) UPLC-MSE profiling of phytoplankton metabolites: application to the identification of pigments and structural analysis of metabolites in Porphyridium purpureum. Mar Drugs 13:2541–2558. https://doi.org/10.3390/md13042541

Juin C, Oliveira Junior RG, Fleury A, Oudinet C, Pytowski L, Bérard JB, Nicolau E, Thiéry V, Lanneluc I, Beaugeard L, Prunier G, Almeida JRGDS, Picot L (2018) Zeaxanthin from Porphyridium purpureum induces apoptosis in human melanoma cells expressing the oncogenic BRAF V600E mutation and sensitizes them to the BRAF inhibitor vemurafenib. Rev Bras 28:457–467. https://doi.org/10.1016/j.bjp.2018.05.009

Kaňa R, Kotabová E, Sobotka R, Prášil O (2012) Non-photochemical quenching in cryptophyte alga Rhodomonas salina is located in chlorophyll a/c antennae. PLoS One 7:e29700. https://doi.org/10.1371/journal.pone.0029700

Kumar SR, Hosokawa M, Miyashita K (2013) Fucoxanthin: a marine carotenoid exerting anti-cancer effects by affecting multiple mechanisms. Mar Drugs 11:5130–5147. https://doi.org/10.3390/md11125130

Lopatka J, Malon K, Kryk M (2018) Hybrid model of radio channels occupancy prediction for dynamic spectrum access. URSI 2018 - Balt URSI Symp 2015:238–241. https://doi.org/10.23919/URSI.2018.8406694

Matthews NH, Li W-Q, Qureshi AA, Weinstock MA, Cho E (2017) Epidemiology of melanoma. In: Ward WH, Farma JM (eds) Cutaneous melanoma: etiology and therapy. Codon Publications, Brisbane (AU), pp 3–22. https://doi.org/10.15586/codon.cutaneousmelanoma.2017.ch1

Mosmann T (1983) Rapid colorimetric assay for cellular growth and survival: application to proliferation and cytotoxicity assays. J Immunol Methods 65:55–63. https://doi.org/10.1016/0022-1759(83)90303-4

Napolitano S, Brancaccio G, Argenziano G, Martinelli E, Morgillo F, Ciardiello F (2018) It is finally time for adjuvant therapy in melanoma. Cancer Treat Rev 69:101–111. https://doi.org/10.1016/j.ctrv.2018.06.003

Pasquet V, Morisset P, Ihammouine S, Chepied A, Aumailley L, Berard JB, Serive B, Kaas R, Lanneluc I, Thiery V, Lafferriere M, Piot JM, Patrice T, Cadoret JP, Picot L (2011) Antiproliferative activity of violaxanthin isolated from bioguided fractionation of Dunaliella tertiolecta extracts. Mar Drugs 9:819–831. https://doi.org/10.3390/md9050819

Porter AG, Ja RU (1999) Emerging roles of caspase-3 in apoptosis. Cell Death Differ 6:99–104

Prado G, Svoboda RM, Rigel DS (2019) What's new in melanoma. Dermatol Clin 37:159–168. https://doi.org/10.1016/j.det.2018.12.005

Ronca R, Di Salle E, Giacomini A, Leali D, Alessi P, Coltrini D, Ravelli C, Matarazzo S, Ribatti D, Vermi W, Presta M (2013) Long pentraxin-3 inhibits epithelial-mesenchymal transition in melanoma cells. Mol Cancer Ther 12:2760–2771. https://doi.org/10.1158/1535-7163.MCT-13-0487

Roos WP, Quiros S, Krumm A, Merz S, Switzeny OJ, Christmann M, Loquai C, Kaina B (2014) B-Raf inhibitor vemurafenib in combination with temozolomide and fotemustine in the killing response of malignant melanoma cells. Oncotarget 5:12607–12620. https://doi.org/10.18632/oncotarget.2610

Sanz N, García-Blanco A, Gavalás-Olea A, Loures P, Garrido JL (2015) Phytoplankton pigment biomarkers: HPLC separation using a pentafluorophenyloctadecyl silica column. Methods Ecol Evol 6:1199–1209. https://doi.org/10.1111/2041-210X.12406

Sathasivam R, Ki JS (2018) A review of the biological activities of microalgal carotenoids and their potential use in healthcare and cosmetic industries. Mar Drugs 16:1–31. https://doi.org/10.3390/md16010026

Schadendorf D, van Akkooi ACJ, Berking C, Griewank KG, Gutzmer R, Hauschild A, Stang A, Roesch A (2018) Melanoma. Lancet 392:971–984. https://doi.org/10.1016/S0140-6736(18)31559-9

Sengupta S, Koley H, Dutta S, Bhowal J (2018) Hypocholesterolemic effect of Spirulina platensis (SP) fortified functional soy yogurts on diet-induced hypercholesterolemia. J Funct Foods 48:54–64. https://doi.org/10.1016/j.jff.2018.07.007

Serive B, Nicolau E, Bérard JB, Kaas R, Pasquet V, Picot L, Cadoret JP (2017) Community analysis of pigment patterns from 37 microalgae strains reveals new carotenoids and porphyrins characteristic of distinct strains and taxonomic groups. PLoS One 12:e0171872. https://doi.org/10.1371/journal.pone.0171872

Spagnolo F, Ghiorzo P, Orgiano L, Pastorino L, Picasso V, Tornari E, Ottaviano V, Queirolo P (2015) BRAF-mutant melanoma: treatment approaches, resistance mechanisms, and diagnostic strategies. Onco Targets Ther 8:157–168. https://doi.org/10.2147/OTT.S39096

Spagnolo F, Ghiorzo P, Queirolo P (2014) Overcoming resistance to BRAF inhibition in BRAF-mutated metastatic melanoma. Oncotarget 5:10206–10221. https://doi.org/10.18632/oncotarget.2602

Sugawara T, Ganesan P, Li Z, Manabe Y, Hirata T (2014) Siphonaxanthin, a green algal carotenoid, as a novel functional compound. Mar Drugs 12:3660–3668. https://doi.org/10.3390/md12063660

Tentori L, Lacal PM, Graziani G (2013) Challenging resistance mechanisms to therapies for metastatic melanoma. Trends Pharmacol Sci 34:656–666. https://doi.org/10.1016/j.tips.2013.10.003

Teubner K, Tolotti M, Greisberger S, Heike M, Dokulil MT, Morscheid H (2003) Steady state phytoplankton in a deep pre-alpine lake: species and pigments of epilimnetic versus metalimnetic assemblages. Hydrobiologia 502:49–64. https://doi.org/10.1023/B:HYDR.0000004269.54705.cb

Tracey EH, Vij A (2019) Updates in melanoma. Dermatol Clin 37:73–82. https://doi.org/10.1016/j.det.2018.08.003

Tremblay R, Cartier S, Miner P, Pernet F, Quéré C, Moal J, Muzellec ML, Mazuret M, Samain JF (2007) Effect of Rhodomonas salina addition to a standard hatchery diet during the early ontogeny of the scallop Pecten maximus. Aquaculture 262:410–418. https://doi.org/10.1016/j.aquaculture.2006.10.009

van Houcke J, Medina I, Maehre HK, Cornet J, Cardinal M, Linssen J, Luten J (2017) The effect of algae diets (Skeletonema costatum and Rhodomonas baltica) on the biochemical composition and sensory characteristics of Pacific cupped oysters (Crassostrea gigas) during land-based refinement. Food Res Int 100:151–160. https://doi.org/10.1016/j.foodres.2017.06.041

Vinod BS, Maliekal TT, Anto RJ (2013) Phytochemicals as chemosensitizers: from molecular mechanism to clinical significance. Antioxid Redox Signal 18:1307–1348. https://doi.org/10.1089/ars.2012.4573

Voskoboynik M, Arkenau HT (2014) Combination therapies for the treatment of advanced melanoma: a review of current evidence. Biochem Res Int 2014:307059. https://doi.org/10.1155/2014/307059

Vu MTT, Douëtte C, Rayner TA, Thoisen C, Nielsen SL, Hansen BW (2016) Optimization of photosynthesis, growth, and biochemical composition of the microalga Rhodomonas salina—an established diet for live feed copepods in aquaculture. J Appl Phycol 28:1485–1500. https://doi.org/10.1007/s10811-015-0722-2

Walne PR (1970) Studies on food value of nineteen genera of algae to juvenile bivalves of the genera Ostrea, Crassostrea, Mercenaria and Mytilus. Fish Invest L Ser 26:1–62

Wang C, Kim J, Kim S (2014) Carotenoids: new opportunities and future prospects. Mar Drugs 12:4810–4832. https://doi.org/10.3390/md12094810

Zapata M, Rodriguez F, Garrido JL (2000) Separation of chlorophylls and carotenoids from marine phytoplankton: a new HPLC method using a reversed phase C_8 column and pyridine-containing mobile phases. MEPS 195:29–45. https://doi.org/10.3354/meps195029